Original Article

Tumor-associated macrophages regulate gastric cancer cell invasion and metastasis through TGFβ2/NF-κB/Kindlin-2 axis

Zhu Wang[1,2], Yang Yang[1,2], Yancheng Cui[1,2,3], Chao Wang[1,2], Zhiyong Lai[1,2], Yansen Li[1,2], Wei Zhang[1,2], Harri Mustonen[3], Pauli Puolakkainen[3], Yingjiang Ye[1,2], Kewei Jiang[1,2], Zhanlong Shen[1,2], Shan Wang[1,2]

[1]Department of Gastroenterological Surgery, Peking University People's Hospital, Beijing 100044, China; [2]Laboratory of Surgical Oncology, Beijing Key Laboratory of Colorectal Cancer Diagnosis and Treatment Research, Peking University People's Hospital, Beijing 100044, China; [3]Department of Surgery, Helsinki University Central Hospital, and University of Helsinki, Helsinki 00290, Finland

Correspondence to: Shan Wang. Department of Gastroenterological Surgery, Peking University People's Hospital, No. 11 Xizhimen South Street, Xicheng District, Beijing 100044, China. Email: shanwang60@sina.com; Zhanlong Shen. Department of Gastroenterological Surgery, Peking University People's Hospital, No. 11 Xizhimen South Street, Xicheng District, Beijing 100044, China. Email: shanwang60@sina.com; Kewei Jiang. Department of Gastroenterological Surgery, Peking University People's Hospital, No. 11 Xizhimen South Street, Xicheng District, Beijing 100044, China. Email: dr_jiangkewei@163.com.

Abstract

Objective: Recent studies have shown that tumor-associated macrophages (TAMs) play an important role in cancer invasion and metastasis. Our previous studies have reported that TAMs promote the invasion and metastasis of gastric cancer (GC) cells through the Kindlin-2 pathway. However, the mechanism needs to be clarified.

Methods: THP-1 monocytes were induced by PMA/interleukin (IL)-4/IL-13 to establish an efficient TAM model *in vitro* and M2 macrophages were isolated via flow cytometry. A dual luciferase reporter system and chromatin immunoprecipitation (ChIP) assay were used to investigate the mechanism of transforming growth factor β2 (TGFβ2) regulating Kindlin-2 expression. Immunohistochemistry was used to study the relationships among TAM infiltration in human GC tissues, Kindlin-2 protein expression, clinicopathological parameters and prognosis in human GC tissues. A nude mouse oncogenesis model was used to verify the invasion and metastasis mechanisms *in vivo*.

Results: We found that Kindlin-2 expression was upregulated at both mRNA and protein levels in GC cells cocultured with TAMs, associated with higher invasion rate. Kindlin-2 knockdown reduced the invasion rate of GC cells under coculture condition. TGFβ2 secreted by TAMs regulated the expression of Kindlin-2 through the transcription factor NF-κB. TAMs thus participated in the progression of GC through the TGFβ2/NF-κB/Kindlin-2 axis. Kindlin-2 expression and TAM infiltration were significantly positively correlated with TNM stage, and patients with high Kindlin-2 expression had significantly poorer overall survival than patients with low Kindlin-2 expression. Furthermore, Kindlin-2 promoted the invasion of GC cells *in vivo*.

Conclusions: This study elucidates the mechanism of TAMs participating in GC cell invasion and metastasis through the TGFβ2/NF-κB/Kindlin-2 axis, providing a possibility for new treatment options and approaches.

Keywords: Gastric cancer; tumor-associated macrophage; Kindlin-2; invasion and metastasis

Submitted May 13, 2019. Accepted for publication Dec 18, 2019.
doi: 10.21147/j.issn.1000-9604.2020.01.09
View this article at: https://doi.org/10.21147/j.issn.1000-9604.2020.01.09

Introduction

Gastric cancer (GC) is the fifth most frequently diagnosed cancer and the third most lethal cancer worldwide (1). Although many treatments for GC have been evaluated, the curative effect is still poor (2,3). Invasion and metastasis are

important factors that affect the prognosis of patients with GC (4). According to the American Surveillance, Epidemiology and End Results (SEER) database, the 5-year survival rate of GC patients is 62.5%, but the percentage of patients with local invasion and distant metastasis has been decreased to 27.0% and 3.4%, respectively (5). However, the molecular mechanism of GC invasion and metastasis remains unclear.

Chronic inflammation induced by inflammatory cells in tumors plays an important role in tumor progression (6). Tumor associated macrophages (TAMs) are an important component of the leukocyte infiltrate, and TAMs and related cell types in mouse and human tumors generally have an M2 phenotype, which is oriented towards promoting tumor growth, remodeling tissues, promoting angiogenesis and suppressing adaptive immunity (7). The M2 phenotype of macrophages may also regulate the invasion and metastasis of various tumors (8-10); however, the mechanisms involved in this process remain unclear. Kindlin-2, a FERM domain-containing protein that contributes to the maturation of focal adhesions through the recruitment of migfilin and filamin (11), is a newly discovered key molecule participating in β1 and β3 integrin activation (12). Our previous study found that Kindlin-2 protein expression was positively correlated with the infiltration depth and lymph node metastasis of GC at the mRNA and protein levels, but negatively correlated with prognosis (13). We also found that the invasive ability of GC cells enhanced by TAMs can be inhibited by interfering with Kindlin-2 expression. Therefore, we speculate that Kindlin-2 may play an important role in TAM-mediated process of GC invasion and metastasis and that this mechanism is worth studying.

This study, we first determined that transforming growth factor β2 (TGFβ2) secreted by TAMs increases the invasive ability of GC cells by promoting Kindlin-2 expression. Then, we investigated the mechanism of the TGFβ2/NF-κB/Kindlin-2 axis signaling pathway. Taken together, our findings provide new insights into the molecular mechanism and treatment of GC.

Materials and methods

Cell lines and cell culture

The human GC cell lines AGS, HGC-27, Hs-746T, and NCI-N87 were purchased from the Cell Bank of the Chinese Academy of Sciences (Shanghai, China) and the human monocyte cell line THP-1 was purchased from the National Infrastructure of Cell Line Resource. All cells were tested and authenticated for their genotypes by DNA fingerprinting. All cell lines were passaged for fewer than 6 months after reconstitution. For TAM/GC coculture, Transwell chambers (24-well plates, 0.4-μm pore size; Corning, New York, USA) were used. GC cells were seeded in the upper chambers and TAMs were placed in the lower wells; a volume of RPMI1640 medium containing 10% fetal bovine serum (FBS) (all from Thermo Fisher Scientific, Waltham, USA) sufficient to fill the lower wells and cover the cells in chambers was added. All experimental cells were cultured in RPMI 1640 medium supplemented with 10% FBS in an incubator with 5% CO_2 at 37 °C.

Isolation of monocytes and macrophages

Mononuclear cells were isolated from the blood of healthy subjects via density gradient centrifugation (Ficoll-Paque, Amersham, Uppsala, Sweden). Three layers were present after density gradient centrifugation, and mononuclear cells located in the second cloudy layer were transferred to a clean tube, washed with a phosphate-buffered saline (PBS) + 10% acid citrate dextrose (ACD) solution and centrifuged twice. The cells were counted and 1.4×10^6 cells were placed on coverslips (Nalge Nunc International Corporation, Naperville, Germany) coated with Matrigel (Matrigel, BD Biosciences, San Jose, USA). The isolated cells were cultured in serum-free medium designed for macrophages (macrophage serum-free medium, Gibco, Paisley, UK) supplemented with granulocyte-macrophage colony stimulating factor [granulocyte-macrophage colony-stimulating factor (GM-CSF); 10 ng/mL, ImmunoTools, Oldenburg, Germany] and antibiotics at 37 °C with 5% CO_2. Monocytes adhered to the Matrigel overnight and differentiated to macrophages due to GM-CSF, and the non-adherent mononuclear cells were removed from the medium next day. The monocytes were fully differentiated into macrophages after 6 d and then used for experiments. When cocultured with cancer cells, macrophages developed into TAMs expressing a special surface marker, CD163.

Quantitative flow cytometry

A total of 5×10^5 cells were stained with an isotype-matched control antibody or a relevant antibody for 1 h at 4 °C in the dark. For indirect immunofluorescence staining, $CD163^+$ macrophages were initially incubated with an

unconjugated primary anti-CD163 antibody (Becton Dickinson, San Jose, USA) for 1 h at 4 °C, washed three times with Dulbecco's phosphate-buffered saline (D-PBS), pH=7.4, and then incubated with a goat anti-mouse Alexa-Fluor 488-conjugated secondary antibody (1:200 dilution; Molecular Probes) for 1 h at 4 °C in the dark. The stained cells were washed twice with D-PBS, pH=7.4, resuspended in 400 μL of FACS-Flow buffer (Becton Dickinson, San Jose, USA), and kept on ice until analysis. All samples were analyzed using a FACS Calibur flow cytometer, and compensation for spectral overlap was ensured using FlowJo for Macintosh software (Version 8.3, TreeStar, San Carlos, USA). For CD163 density quantification, flow cytometric estimation of antibodies bound per cell (ABC) was performed using Quantibrite PE beads (Becton Dickinson, Heidelberg, Germany) as recommended by the manufacturer. After the cells were stained as described, a set of 4 precalibrated fluorescence-labeled beads were used for standardization before the samples were acquired. The Quantibrite PE beads were run at the same instrument settings used for the assay, and the linear regression obtained using the Quantibrite PE beads was used to convert the FL2 linear fluorescence staining of the cell population into the number of (CD163) PE molecules bound per cell. CD11b, CD68, CD86 and CD206 were detected via the same method and all antibodies were obtained from Becton Dickinson (San Jose, CA, USA).

RNA extraction and purification

Total RNA was extracted from tissue samples or cell lines using the RNeasy Mini Kit (QIAGEN, Hilden, Germany) and purified using an RNase-Free DNase Set (QIAGEN) according to the manufacturer's protocol. The purity and concentration of the RNA were determined from OD260/280 readings using a spectrophotometer (Nano-Drop ND-1000). RNA integrity was determined by 1% formaldehyde denaturing gel electrophoresis.

Real-time quantitative polymerase chain reaction (RT-qPCR)

Total RNA was used for reverse transcription, which was performed at 37 °C for 60 min with a Quantscript RT Kit (KR103; Tiangen Biotechnology, Beijing, China). All samples were quantified after PCR amplification using a RealMasterMix (SYBR Green) kit (FP202; Tiangen Biotechnology). The primer sequences are shown in *Table 1*. The PCR protocol was as follows: initial denaturation at 95 °C for 10 min, followed by 30 cycles at 95 °C for 10 s, annealing at 58.5 °C for 5 s, and extension at 72 °C for 8 s. PCR products were quantified via melting curves at 84 °C. All results were normalized to β-actin to ensure a uniform amount of RNA template.

RNA interference

Gene silencing was performed by transfecting AGS cells with siRNA oligonucleotides (GenePharma, Shanghai, China). The siRNA sequences are shown in *Table 2*. For transfections in 12-well plates, 1.0×10^5 cells were seeded per well overnight, and then transfected with 80 nmol/L target siRNA or negative control sequence using Lipo2000

Table 1 PCR primers used in this study

Gene name	Forward primer (5' → 3')	Reverse primer (5' → 3')
IL-8	TGCCAAGGAGTGCTAAAG	CTCCACAACCC TCTGCAC
IL-11	TGCGTCGACATGAACTGTGTTTGCCGC	ATGAAGCTTTGGAAGGACGGTGGTGGC
TNFSF7	TGGTGATCTCCCTCCTGGTG	GCACCCACTGCACTCCAAAG
MMP-9	AAGGTCGCTCGGATGGTTAT	AGTTGCCCCCAGTTACAGTG
VEGF-A	GAGGCGCAGCGGTTAGGTGGAC	GGCTCCTCCGAAGCGAGAACA
VEGF-C	CAGCACGAGCTACCTCAGCAAG	TTTAGACATGCATCGGCAGGAA
β1-integrin	TTGCCTTGCTGCTGATTTGG	AGTTGTCACGGCACTCTTGT
NF-κB	AGTTGAGGGGACTTTCCCAGGC	GCCTGGGAAAGTCCCCTCAACT
TGF-β	AACTACTGCTTCAGCTCCAC	TGTGTCCAGGCTCCAAATGTA
Kindlin-2	AAATGGTCACCGTAGAGTTTGC	CTCTCGTTTTGGTCTTTTGCAC
β-actin	AAGGTGACAGCAGTCGGTT	AAGTGGGGTGGCTTTTAG

PCR, polymerase chain reaction; IL, interleukin; TNFSF7, tumor necrosis factor (ligand) superfamily, member 7; MMP, matrix metalloprotein; VEGF, vascular endothelial growth factor; TGF, transforming growth factor.

Table 2 siRNA sequences used in this study

Identifier	Sense primer sequence (5' → 3')	Anti-sense primer sequence (3' → 5')
Kindlin-2 siRNA	GCUGGUGGAGAAACUCGAUTT	AUCGAGUUUCUCCACCAGCTT
NF-κB siRNA	GCCCUAUCCCUUUACGUCATT	UGACGUAAAGGGAUAGGGCTT
Control siRNA	UUCUCCGACGUGUCACGUTT	ACGUGACACGUCGGAGAATT

Transfection Agent (Invitrogen, Carlsbad, USA) according to the manufacturer's protocol. In 24–48 h after transfection, cells were harvested or incubated further for the following experiments.

Western blot analysis

GC cells and cocultured cells were lysed in radioimmunoprecipitation assay (RIPA) buffer (Thermo Fisher, Rockford, USA) containing 1% phenylmethane sulfonyl fluoride (PMSF), and the protein concentration was measured using a BCA protein assay kit (Beyotime, Shanghai, China). Fifty micrograms of protein was separated on an 8%–12% sodium dodecyl sulfate-polyacrylamide gel electrophoresis (SDS-PAGE) gel (Beyotime, Shanghai, China) and transferred onto a polyvinylidene difluoride (PVDF) membrane (Bio-Rad, Hercules, USA). The membrane was then blocked with 5% nonfat milk and incubated with anti-Kindlin-2 (1:5,000 dilution; cat. no.ab74030), anti-NF-κB (1:5,000 dilution; cat. no.ab16502) and GAPDH (1:1,000 dilution; cat. no. ab8245; all Abcam, Cambridge, UK) antibodies, followed by incubation at 37 °C for 1 h with a horseradish peroxidase-conjugated secondary antibody (1:2,000 dilution, Beyotime, Shanghai, China). The membrane was stained with ECL Plus (Beyotime, Shanghai, China) according to the manufacturer's instructions.

Transwell matrigel invasion assay

For the matrigel invasion assay, Transwell chambers (24-well plates, 8-μm pore size; Corning) were coated with 100 μL of Matrigel (5 mg/mL) (BD Biosciences, San Jose, USA). Briefly, a total of 1×10^5 cells were seeded in the upper chambers in medium containing 0.1% bovine serum albumin, while medium containing 30% FBS was placed in the lower wells. After 24 h incubation at 37 °C, the non-invading cells were removed with a cotton swab. Invaded cells on the bottom of the membrane were fixed with 1% formalin, stained with 0.1% crystal violet and counted in five randomized fields under a microscope (Olympus Corporation, Tokyo, Japan) at 200× magnification. The Transwell Matrigel invasion assay was repeated three times with technical duplicates.

Evaluation of immunohistochemical staining

The immunohistochemical staining results were assessed by evaluating the mean score for both the intensity of staining and the proportion of tumor cells with an unequivocal positive reaction. Each section was assessed independently by 2 pathologists blinded to the patient data. Positive reactions were defined as those showing brown signals in the cytoplasm. The staining index was determined by multiplying the staining intensity score by the positive area score. The staining intensity score is as follows: 0, negative; 1, weak; 2, moderate; and 3, strong. The proportion of positive cells is defined as follows: 0, less than 5%; 1, 6%–25%; 2, 26%–50%; 3, 51%–75%; and 4, greater than 75%. For statistical analysis, we used the K-adaptive partitioning statistical (KAPS) algorithm in R software (Version 3.2.5; R Foundation for Statistical Computing, Vienna, Austria) to calculate the most efficient cut-off value. Cases with a score below the cut-off value were considered low expression, while cases with a score above the cut-off value are considered to show high expression.

Luciferase reporter assay

Two plasmid vectors were constructed: the dual-luciferase PGL-3 K2 wild-type (WT) vector containing the *Kindlin-2* gene promoter (promoter region sequence from the transcription start site to 2,000 bp upstream) and the dual-luciferase PGL-3 K2 mutant (Mut) vector containing a mutated NF-κB promoter region (lacking the NF-κB binding site: −468 bp to −453 bp, CTGGGAATTTC CTGG promoter region). AGS cells were seeded at 5×10^4 cells/well in 24-well plates overnight, and then were cotransfected with PGL-3 K2 Mut, PGL-3 K2 WT, and empty PGL-3 vectors accordingly. Forty-eight hours after transfection, the cells were lysed using passive lysis buffer (Promega, Madison, USA), and the luciferase activity was measured by a GloMax20/20 luminometer (Promega) using the Dual Luciferase Reporter Assay System (Promega) and normalized to Renilla luciferase activity. The experiments were performed in triplicate.

Nude mouse oncogenesis model

This experiment was conducted at Crown Bioscience and received ethical approval from the Committee on the Ethics of Animal Experiments of Crown Bioscience [Crown Bioscience Institutional Animal Care and Use Committee (IACUC)]. The animal maintenance, handling and experimental procedures followed were in accordance with the Guidelines for the Care and Use of Laboratory Animals of the National Institutes of Health.

Adult female BALB/c nude mice (18–22 g) were obtained from Anikeeper (Beijing, China). The animals were acclimatized to standard housing conditions (23±3 °C, 40%–70% relative humidity, 12 h light-dark cycle with lights on at 07:00), with free access to water and chow diet, for one week before the experiment. Each mouse was inoculated subcutaneously in the right front subaxillary region with tumor cells (1×10^7) in 0.1 mL of PBS.

In the pre-experiment, six mice were divided into three groups, namely Kindlin-2 overexpression group, Kindlin-2 normal expression group and inhibitor alone (SB431542 adding) group (named group α, β and γ, respectively), and observed the tumor growth in different groups.

In the formal experiment, eigthteen mice were randomly allocated to three study groups. Mice in group 01 and 03 were injected subcutaneously with pL/shGFP-NC (Kindlin-2$^+$) cells, and mice in group 02 were injected subcutaneously with pL/shGFP-Kindlin-2 (Kindlin-2$^-$) cells. Tumor growth was monitored twice a week using a caliper. Animals in group 01 and 02 were injected subcutaneously with TGFβ2 (0.1 μg/mouse; Cell signaling technology, Boston, USA) dissolved in 20 mmol/L citrate once a week, while group 03 mice received an injection of SB431542. When the tumor sizes reached 100–200 mm^3 (1/2 length×width^2), the tumor volume and body weight were recorded, and the first recorded date was d 0. When the average tumor size reached 2,000 mm^3, tumors were harvested for subsequent histopathology and immunohistology analysis.

Chromatin immunoprecipitation (ChIP) assay

A total of 5×10^6 cells were cultured in each 10-cm dish and subjected to the following protocol: Rinse the cells twice with PBS. Add 5 mL 1% formaldehyde in PBS to the cells and incubate for 10 min at room temperature. Add 550 μL 1.25 mol/L glycine, swirl gently to mix and incubate for 5 min. Aspirate the supernatant and wash the pellet with PBS 2 times. Prepare the sonication buffer/protease inhibitors and add 0.5 mL of the mixture to each plate. After 1 min, scrape the cells with a sterile scraper. Pipet the suspension into a 2-mL Eppendorf tube and place the tube on wet ice for 10 min. Sonicate 10–15 times with 10 s pulses. Place the tube on dry ice followed by wet ice for 1–2 min after each pulse. Verify chromatin fragmentation by running 8 μL of the sample on a 1% agarose gel. Centrifuge the sample in a refrigerated microfuge for 10–15 min at the highest speed. Aliquot 25 μL of the sonicated sample as the input. Mix 250 μL sonicated sample with 555 μL dilution buffer containing protease inhibitor cocktail, and then add 50 μL of magnetic bead-coupled anti-rabbit IgG and incubate for 30 min at 4 °C with rotation. After absorbing the magnetic beads with a magnetic separation rack for 2 min, aliquot the supernatant into two groups: IP and neg. Add 5 μg of anti-NF-κB to the IP tubes and incubate with the neg tubes overnight with rotation. Adsorb the magnetic beads with the magnetic separation rack two times for 2 min each. Use ChIP elution buffers/proteinase K to elute the samples for 2 h at 62 °C. Add RNase and incubate for 20 min at 37 °C, followed by 10 min at 95 °C. Add a mixture of phenol/chloroform/isoamyl alcohol (25:24:1) and centrifuge the sample for 10–15 min at a speed of 10,783 r/min at 4 °C. Transfer the supernatant to fresh Eppendorf tubes and add 30 μg of glycogen, 1 mL of absolute ethyl alcohol, and 5 mol/L NaCl to a final concentration of 200 mmol/L. After incubating the samples for 30 min at −80 °C, centrifuge the samples for 20 min at a speed of 10,783 r/min at 4 °C to precipitate the DNA. Wash the DNA with 500 μL of 70% ethyl alcohol. After air drying the precipitate, dissolve it in 20 μL of 10 mmol/L Tris-HCl pH 8.0. PCR was used to evaluate the expression of Kindlin-2 in the three groups, and 8 μL of the PCR product was run on a 1% agarose gel.

Statistical analysis

Data analysis was performed using the SPSS software (Version 22.0, IBM Corp., New York, USA). Non-parametric tests were used to compare Kindlin-2 expression in tumor tissues and paraneoplastic tissues. Differences in Kindlin-2 expression and clinicopathologic variables were compared using the Fishers' exact test or the Cochran-Armitage trend test in the case of ordered categories. The overall survival (OS) time was calculated from the date of surgery to the last follow-up assessment or the day of death. The median survival follow-up was 46.6 (range, 2.0–99.0) months. Univariate analysis was conducted using

the Kaplan-Meier method, and survival times were compared using the log-rank test. The Cox proportional hazards model was used for multivariate analysis. P<0.05 on both sides were considered statistically significant.

Results

TMAs increased invasive ability of GC cells through TGFβ2

THP-1 monocytes were used for macrophages differentiation. THP-1 monocytes were differentiated into M1 macrophages with 6 h PMA stimulation followed by lipopolysaccharide (LPS) + interferon (IFN)-γ treatment for 18 h, while M2 macrophages were collected after stimulation with PMA for 6 h followed by interleukin (IL)-4 + IL-13 treatment for 18 h. The expression of surface antigens, such as CD163 (86.45±2.13 *vs*. 34.05±5.56, P<0.001), CD206 (76.82±2.84 *vs*. 16.53±5.97, P<0.001), and CD11b (90.69±1.89 *vs*. 12.48±3.39, P<0.001), was significantly higher in M2 macrophages than in M1 macrophages. In contrast, CD86 (6.95±2.79 *vs*. 18.78±2.72, P<0.001) expression was significantly lower in M2 macrophages than in M1 macrophages, and the expression of CD68 (75.89±4.74 *vs*. 92.70±1.61, P=0.061) was not significantly different between two groups (*Figure 1A*). In the following studies, we used M2 macrophages, and unless otherwise stated, TAMs specifically target M2 macrophages.

We examined the Kindlin-2 mRNA expression and the invasive ability of GC cells in two groups: a TAM/GC coculture group and a conventional GC cell-only group. The relative Kindlin-2 mRNA expression level of TAM/GC and GC groups were 4.74±0.35 and 1.00±0.18, respectively (P<0.001) and the related cell invasive ability of these two groups were (258.3±8.2)% and (100.0±6.5)%, respectively (P<0.001). After downregulating Kindlin-2 expression in GC cells using siRNA and incubating GC cells with TAMs, the relative Kindlin-2 mRNA expression [0.22±0.06 *vs*. 4.74±0.35 for TAM/GC siRNA-Kindlin-2 (siK2) and TAM/GC groups, respectively, P<0.001] and invasive ability [(212.67±14.38)% *vs*. (258.33±8.22)%, P=0.029] promoted by TAMs were significantly decreased (*Figure 1D–F*).

To investigate the intrinsic mechanism, we identified four cytokines significantly increased in the TAM/GC coculture group using cytokine chips (Human Common Cytokines PCR Array, QIAGEN) and RT-qPCR [normalized to the GC alone group: tumor necrosis factor (ligand) superfamily, member 7 (TNFSF7), 39.8±1.1, P<0.05; TGFβ2, 16.9±0.4, P<0.05; IL-8, 28.8±2.3, P<0.05; IL-11, 31.2±1.7, P<0.05] (*Figure 1B*). Moreover, the TGFβ receptor inhibitor (SB431542) reduced the relative expression of Kindlin-2 mRNA (relative to the TAM/GC group: 0.6±0.0, P=0.001), β1-integrin (0.5±0.0, P<0.001), matrix metalloprotein (MMP)-9 (0.7±0.0, P=0.006), vascular endothelial growth factor (VEGF)-A (0.4±0.0, P=0.004), and VEGF-C (0.3±0.0, P<0.001) (*Figure 1C*).

Next we explored the effect of TGFβ2 on the invasion and metastasis of GC cells, RT-qPCR was used to examine the Kindlin-2 mRNA expression in GC cells among six different groups. TGFβ2 treatment for 24 h significantly increased Kindlin-2 mRNA expression in GC cells (5.33±0.32 *vs*. 1.00±0.18, P<0.001), similar to the effect observed in the TAM/GC coculture group. The TGFβ receptor inhibitor SB431542 decreased the Kindlin-2 mRNA upregulation in the TAM/GC cell coculture group (4.74±0.35 *vs*. 3.77±0.32, P=0.017). Similar results were acquired using another TGFβ receptor inhibitor, LY2157299 (*Supplementary Figure S1A*). Furthermore, SB431542 further reduced Kindlin-2 mRNA expression in the TAM/GC (siK2) group (0.15±0.02 *vs*. 0.22±0.03, P=0.020) (*Figure 1D*). Moreover, consistent results were obtained for Kindlin-2 protein expression (*Figure 2B*).

The transwell invasion assay was used to examine the invasive ability of GC cells. TGFβ2 treatment for 24 h significantly increased the cell invasive ability of GC cells [183.0±10.9)% *vs*. (100.0±6.5)%, P<0.001], similar to the effect observed in the TAM/GC coculture group. The TGFβ receptor inhibitor SB431542 decreased the GC cells invasive ability of the TAM/GC cell coculture group [(258.3±8.2)% *vs*. (226.7±11.1)%, P=0.011]. After adding SB431542 to the TAM/GC (siK2) group, the invasive ability of the GC cells [(205.2±10.2)% *vs*. (130.2±0.03)%, P<0.001] got decreased further (*Figure 1E,F*). Moreover, consistent results were obtained in the migration assay (*Supplementary Figure S1C*), and the cell wound scratch assay also showed similar results (*Supplementary Figure S1B*).

TGFβ regulated expression of Kindlin-2 through transcription factor NF-κB

Using bioinformatics software, we analyzed possible regulatory factors that could affect the expression of *Kindlin-2* gene and the target range located from 2,000 bp upstream to 2,000 bp downstream of its transcription start site. There were eight transcription factors predicted by

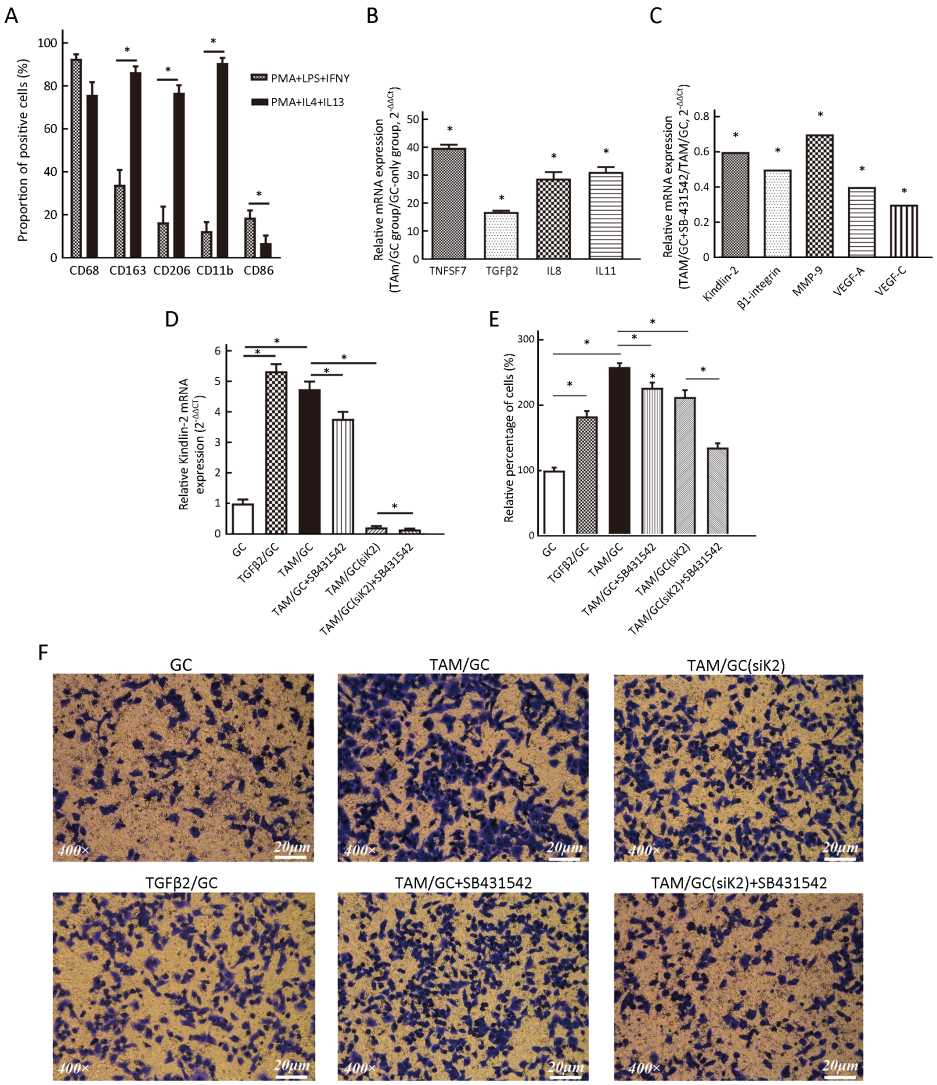

Figure 1 Tumor-associated macrophages (TAMs) increased invasive ability of gastric cancer (GC) cells through transforming growth factor β2 (TGFβ2). (A) CD163, CD206 and CD11b expression levels were significantly higher in M2 macrophages than in M1 macrophages (CD163, 86.45±2.13 *vs*. 34.05±5.56, P<0.001; CD206, 76.82±2.84 *vs*. 16.53±5.97, P<0.001 and CD11b, 90.69±1.89 *vs*. 12.48±3.39, P<0.001). CD86 was significantly higher in M1 macrophages than in M2 macrophages (CD86, 6.95±2.79 *vs*. 18.78±2.72, P<0.001), and CD68 expression was not significantly different between the two groups (CD68, 75.89±4.74 *vs*. 92.70±1.61, P=0.061); (B) Tumor necrosis factor (ligand) superfamily, member 7 (TNFSF7), TGFβ2, interleukin (IL)-8 and IL-11 expression levels were significantly increased in the TAM/GC coculture group (TNFSF7, 39.8±1.1, P<0.05; TGFβ2, 16.9±0.4, P<0.05; IL-8, 28.8±2.3, P<0.05; IL-11, 31.2±1.7, P<0.05); (C) Kindlin-2, β1 integrin, matrix metalloprotein (MMP)-9, vascular endothelial growth factor (VEGF)-A and VEGF-C expression levels decreased by SB431542 under TAM/GC condition (Kindlin-2 mRNA, 0.6±0.0, P=0.001; β1-integrin, 0.5±0.0, P<0.001; MMP-9, 0.7±0.0, P=0.006; VEGF-A, 0.4±0.0, P=0.004 and VEGF-C, 0.3±0.0, P<0.001); (D) Comparison of Kindlin-2 mRNA expression among GC, TAM/GC, TAM/GC(siK2), TGFβ2/GC, TAM/GC+SB431542, and TAM/GC(siK2)+SB431542 groups (GC, 1.00±0.18; TAM/GC, 4.74±0.35; TAM/GC(siK2), 0.22±0.03; TGFβ2/GC cells, 5.33±0.32; TAM/GC+SB431542, 3.77±0.32 and TAM/GC(siK2)+SB431542, 0.15±0.02, P<0.001); (E,F) Invasion assay comparing the cell invasive ability among GC, TAM/GC, TAM/GC (siK2), TGFβ2/GC, TAM/GC+SB431542, and TAMs/GC(siK2)+SB431542 groups [GC, (100.0±6.5)%; TAM/GC, (258.3±8.2)%; TAM/GC(siK2), (205.2±10.2)%; TGFβ2/GC cell, (183.0±10.9)%; TAM/GC+SB431542, (226.7±11.1)% and TAM/GC(siK2)+SB431542, (130.2±0.03)%, P<0.001] (×400). *, P<0.001. LPS, lipopolysaccharide; IFN, interferon.

TFSEARCH (with a threshold score of 95 points) and seven transcription factors predicted by JASPSCAN (score of 100 points) that might regulate *Kindlin-2* gene transcription (*Figure 2A*). NF-κB was displayed in both analyses, and NF-κB could participate in many chronic inflammatory and cancer signaling pathways (14); thus, NF-κB was selected for subsequent research.

To elucidate the role of NF-κB in the GC process, we designed four different groups of GC, TGFβ2/GC, TAM/GC, and TAMs/GC+SB431542 to detect the expression of NF-κB mRNA. We found that both TGFβ2/GC (1.35±0.07 *vs*. 1.00±0.14, for the TGFβ2/GC and GC groups, respectively, P=0.012) and the TAM/GC coculture (1.55±0.09 *vs*. 1.00±0.14, for the TAM/GC and GC groups, respectively, P=0.002) significantly increased the NF-κB expression. Furthermore, SB431542 reduced the expression of NF-κB under the TAM/GC coculture condition (0.74±0.08 *vs*. 1.55±0.09, P<0.001). Consistent results were obtained in the protein level of NF-κB (*Figure 2B*).

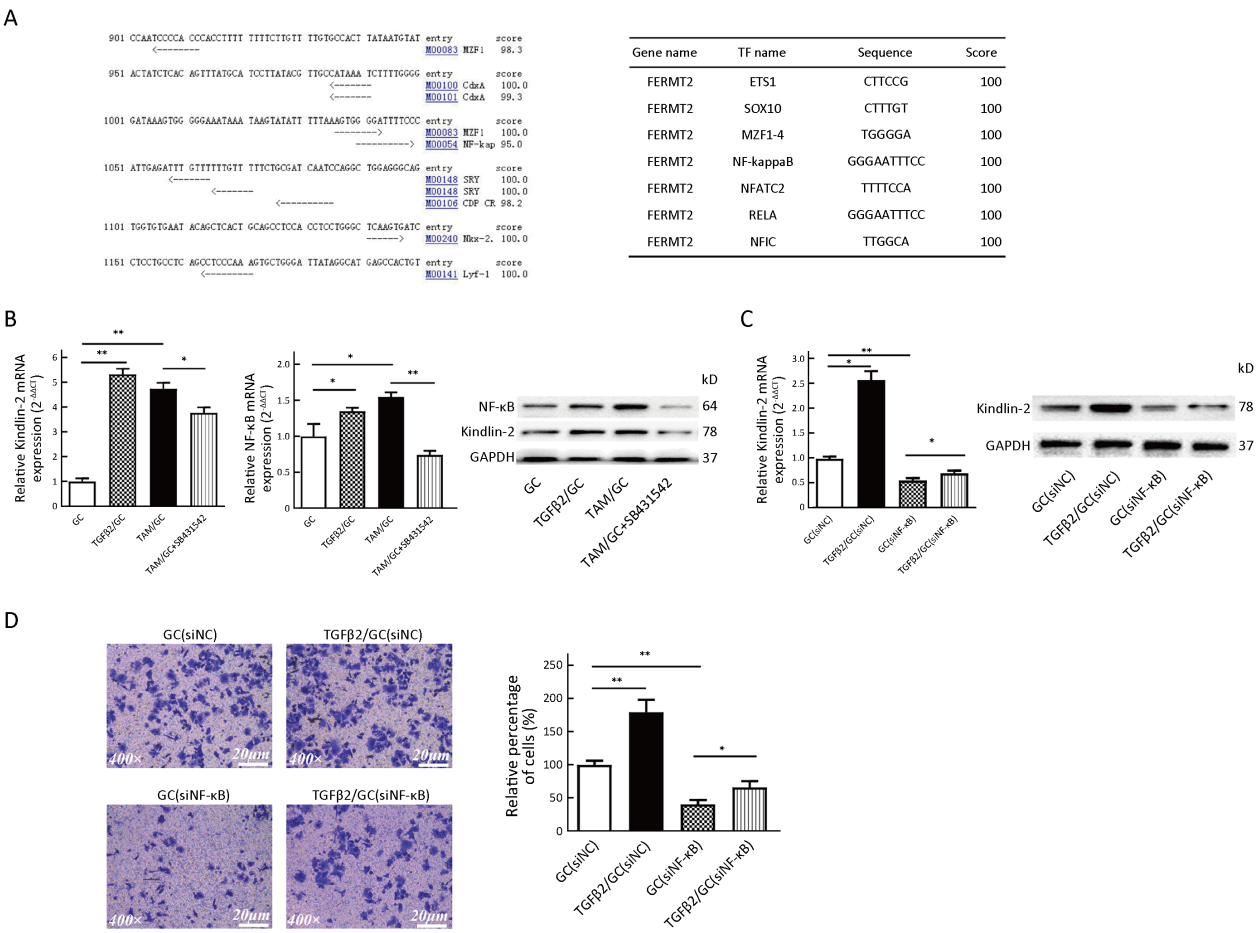

Gene name	TF name	Sequence	Score
FERMT2	ETS1	CTTCCG	100
FERMT2	SOX10	CTTTGT	100
FERMT2	MZF1-4	TGGGGA	100
FERMT2	NF-kappaB	GGGAATTTCC	100
FERMT2	NFATC2	TTTTCCA	100
FERMT2	RELA	GGGAATTTCC	100
FERMT2	NFIC	TTGGCA	100

Figure 2 Transforming growth factor β2 (TGFβ2) regulated expression of Kindlin-2 through transcription factor NF-κB. (A) Transcription factor predicting bioinformatics software, TFSEARCH and JASPSCAN were used to predict the probable transcription factors by different standards (TFSEARCH, with a threshold score of 95 points; JASPSCAN, score of 100 points); (B) Comparison of Kindlin-2 and NF-κB expression at the mRNA and protein levels among the gastric cancer (GC), TGFβ2/GC, TAM/GC, and TAM/GC+SB431542 groups. (NF-κB mRNA: GC, 1.00±0.14; TGFβ2/GC, 1.35±0.07; TAM/GC, 1.55±0.09 and TAM/GC+SB431542, 0.74±0.08, P<0.001); (C) Comparison of Kindlin-2 expression at the mRNA and protein levels among the GC(siNC), TGFβ2/GC(siNC), GC(siNF-κB), and TGFβ2/GC(siNF-κB) groups. [GC(siNC), 0.98±0.04; TGFβ2/GC(siNC), 2.57±0.14; GC(siNF-κB), 0.54±0.04 and TGFβ2/GC(siNF-κB) 0.68±0.04, P<0.001]; (D) Comparison of the cell invasive ability among the GC(siNC), TGFβ2/GC(siNC), GC(siNF-κB), and TGFβ2/GC(siNF-κB) groups [GC(siNC), (100.7±4.9)%; TGFβ2/GC(siNC), (179.7±15.4)%; GC(siNF-κB), (41.3±4.9)% and TGFβ2/GC(siNF-κB), (66.7±7.5)%, P<0.001] (×400). *, P<0.05; **, P<0.001.

NF-κB siRNA was used to knock down NF-κB expression, and Kindlin-2 expression was examined in four groups of GC cells: GC+negative control siRNA (siNC), TGF2β/GC (siNC), GC+NF-κB siRNA (siNF-κB) and TGFβ2/GC (siNF-κB) groups. The results showed that the expression of Kindlin-2 decreased appreciably after NF-κB knockdown [0.54±0.04 *vs*. 0.98±0.04 for the GC(siNF-κB) and GC(siNC) groups, respectively, P<0.001], or after TGFβ2 treatment, and that the expression of Kindlin-2 increased in TGFβ2/GC(siNC) group (2.57±0.14 *vs*. 0.98±0.04, P<0.001) and the TGF2β/GC(siNF-κB) group (0.68±0.04 *vs*. 0.54±0.04, P=0.008) (*Figure 2C*). Moreover, consistent results were observed for the invasion experiments: the invasive ability of GC cells decreased by NF-κB knockdown [(100.7±4.9)% *vs*. (41.3±4.9)%, P<0.001] or TGFβ2 treatment, and the invasive ability increased by TGF2β in both TGF2β/GC(siNC) group [(179.7±15.4)% *vs*. (100.7±4.9)%, P<0.001] and TGF2β/GC(siNF-κB) group [(66.7±7.5)% *vs*. (41.3±4.9)%, P=0.005](*Figure 2D*).

Binding sites of transcription factor NF-κB in Kindlin-2 gene promoter region

To accurately define the binding sites, we constructed two plasmid vectors: a dual-luciferase PGL-3 K2 WT vector containing the WT Kindlin-2 promoter region (promoter region sequence from the transcription start site to 2,000 bp upstream) and a dual-luciferase PGL-3 K2 Mut vector containing a mutated Kindlin-2 promoter region (lacking the NF-κB binding site: −468 bp to −453 bp, CTGG GAATTTCCTGG promoter region) (*Figure 3A*). Then we transfected these vectors into GC cells and detected the luciferase/Renilla fluorescein relative light unit (RLU) ratio after 48 h. Compared with that in the K2 WT group, the dual-luciferase activity ratio in the PGL-3 K2 WT group increased significantly (1.227±0.080 *vs*. 0.999±0.143, P=0.010), while this ratio decreased in the PGL-3 K2 Mut group (0.795±0.084 *vs*. 0.999±0.143, P=0.016) (*Figure 3B*). Furthermore, the ChIP assay using anti-NF-κB confirmed that NF-κB can bind to Kindlin-2 promoter region (*Figure 3C*, *Supplementary Figure S2A,B*).

CD163 and Kindlin-2 were overexpressed in GC tissues, and high expression of CD163 and Kindlin-2 was positively associated with TNM stage and poor prognosis in GC patients

To establish the pathological significance and clinical

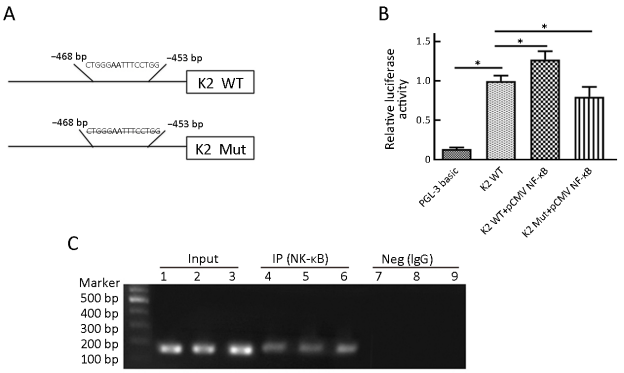

Figure 3 Explored binding sites of transcription factor NF-κB in *Kindlin-2* gene promoter region. (A) Two plasmid vectors were constructed: a dual-luciferase PGL-3 K2 wild-type (WT) vector (containing the WT Kindlin-2 promoter region) and a dual-luciferase PGL-3 K2 mutant (Mut) vector (lacking the NF-κB binding site: −468 bp to −453 bp promoter region); (B) The dual luciferase activity ratio increased significantly in the PGL-3 K2 WT group (1.227±0.080 *vs*. 0.999±0.143, P=0.010), but decreased in the PGL-3 K2 Mut group (0.795±0.084 *vs*. 0.999±0.143, P=0.016); (C) Obvious bands appeared between 100−200 bp in the immunoprecipitation (IP) group, which contained DNA fragments pulled-down by anti NF-κB in the ChIP assay. *, P<0.05.

relevance of Kindlin-2 in GC patients, immunohistochemical staining assays for CD68, CD163, TGFβ2 and Kindlin-2 were performed on tissue microarrays containing 180 tissues from 100 GC patients (80 pairs of cancer/normal tissues, along with another 20 cancer tissues), with a median survival time of 46.6 (range, 2.0−99.0) months. The immunohistochemical staining score, accounting for both the intensity of staining and the proportion of tumor cells with an unequivocal positive reaction, was calculated for each tissue. The expression of CD163 (42.00% *vs*. 26.25%, P=0.029) and Kindlin-2 (54.00% *vs*. 21.25%, P<0.001) was higher in GC tissues than in normal tissues, while the protein level of CD68 (46.00% *vs*. 57.50%, P=0.125) and TGFβ2 (35.00% *vs*. 30.00%, P=0.478) was not significantly different between the two groups (*Figure 4A*,*B*, *Table 3*).

The KAPS algorithm in R software was used to calculate the most efficient cut-off values for the expression of four proteins (15-17), and we found that CD163 (cut-off value=3, P=0.016), TGFβ2 (cut-off value=3, P=0.007) and Kindlin-2 (cut-off value=4, P<0.001) could significantly distinguish the outcomes of these GC patients. A univariate analysis showed that high expression of CD163 (P=0.019) and Kindlin-2 (P=0.025) was positively associated with higher tumor burden as defined by TNM stage (*Table 4*).

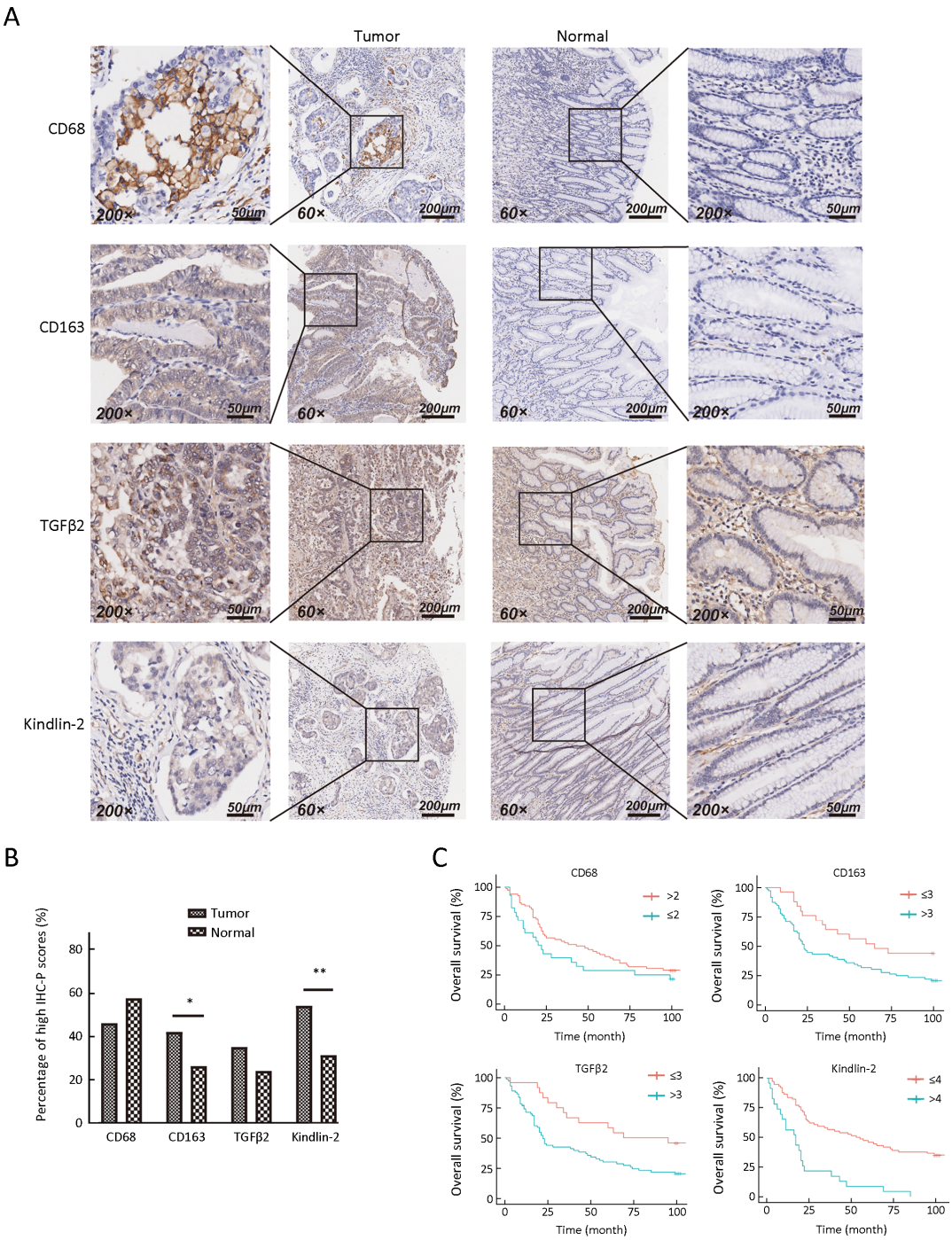

Figure 4 CD163 and Kindlin-2 were overexpressed in gastric cancer (GC) tissues and high CD163 and Kindlin-2 expression was positively associated with TNM stage and poor prognosis in GC patients. (A) Immunohistochemical staining for CD68, CD163, TGFβ2 and Kindlin-2. (×60, ×200); (B) CD163 and Kindlin-2 expression levels were higher in GC tissues than in normal tissues, while CD68 and TGFβ2 expression levels were not significantly different between the two groups, as determined by comparing the immunohistochemical staining scores (CD163, 42.00% *vs*. 26.25%, P=0.029; Kindlin-2, 54.00% *vs*. 21.25%, P<0.001; CD68, 46.00% *vs*. 57.50%, P=0.125 and TGFβ2, 35.00% *vs*. 30.00%, P=0.478); (C) Reduced overall survival (OS) was positively associated with high expression levels of CD163, TGFβ2 and Kindlin-2 in GC patients (CD163, cut-off value=3, P=0.016; TGFβ2, cut-off value=3, P=0.007 and Kindlin-2, cut-off value=4, P<0.001). *, P<0.001; **, P<0.05.

Table 3 Comparative analyses of four protein expression levels in tumor and normal tissues

Protein	Cases (n)	Low [n (%)]	High [n (%)]	χ^2	P
CD68				2.352	0.125
Tumor	100	54 (54.00)	46 (46.00)		
Normal	80	34 (42.50)	46 (57.50)		
CD163				4.846	0.029
Tumor	100	58 (58.00)	42 (42.00)		
Normal	80	59 (73.75)	21 (26.25)		
TGFβ2				0.504	0.478
Tumor	100	65 (65.00)	35 (35.00)		
Normal	80	56 (70.00)	24 (30.00)		
Kindlin-2				19.957	<0.001
Tumor	100	46 (46.00)	54 (54.00)		
Normal	80	63 (78.75)	17 (21.25)		

TGFβ2, transforming growth factor β2.

Furthermore, a Kaplan-Meier survival analysis indicated that reduced OS was positively associated with high expression levels of CD163 (P=0.016), TGFβ2 (P=0.007) and Kindlin-2 (P<0.001) in GC patients (*Figure 4C*), and the multivariate analysis revealed that Kindlin-2 (P<0.001) was an independent prognostic parameter for OS (*Table 5*).

Invasion mechanisms were verified in vivo in a nude mouse oncogenesis model

Stably transfected Kindlin-2 knockdown cell lines were generated containing green fluorescence. The expression of Kindlin-2 was significantly higher in the stably transfected group 02 (Kindlin-2$^-$) than the negative control group 01 (Kindlin-2$^+$) (1.00±0.02 *vs.* 0.23±0.09, P<0.001) (*Figure 5A*).

A nude mouse oncogenesis model was used to evaluate the effect of Kindlin-2 on GC invasion and metastasis *in*

Table 4 Correlation analyses of CD163 and Kindlin2 expression in relation to clinicopathological characteristics of 100 GC patients

Characteristics	Cases (n)	CD163 expression		χ^2	P	Kindlin-2 expression		χ^2	P
		Low (n)	High (n)			Low (n)	High (n)		
Age (year)				5.198	0.023			1.412	0.235
≤65	50	18	32			41	9		
>65	50	8	42			36	14		
Gender				9.215	0.003			0.127	0.722
Female	36	3	33			27	9		
Male	64	23	41			50	14		
Tumor size (cm)				0.014	0.906			0.514	0.473
≤5	51	13	38			32	9		
>5	49	13	36			35	14		
Differentiation				5.486	0.064			1.059	0.589
High	16	3	13			12	4		
Middle	49	9	40			36	13		
Low	35	14	21			29	6		
T stage				1.433	0.231			2.061	0.151
T1–T2	19	7	12			17	2		
T3–T4	81	19	62			60	21		
N stage				2.342	0.126			0.013	0.911
N0	27	10	17			21	6		
N+	73	16	57			56	17		
M stage				0.824	0.364			1.032	0.310
M0	92	25	67			72	20		
M+	8	1	7			5	3		
TNM stage				5.506	0.019			5.034	0.025
I–II	42	16	26			37	5		
III–IV	58	10	48			40	18		

GC, gastric cancer.

Table 5 Univariate and multivariate Cox regression analyses of effect of CD163 and Kindlin-2 expression on OS of GC patients included in tissue array

Characteristics	Univariate analysis			Multivariate analysis		
	HR	95% CI	P	HR	95% CI	P
Age (year)			0.452			–
≤60	1			–	–	
>60	1.010	0.984–1.037		–	–	
Gender			0.841			–
Female	1			–	–	
Male	0.952	0.590–1.538		–	–	
T stage			0.009			0.288
T1–T2	1			1		
T3–T4	2.562	1.269–5.174		1.505	0.708–3.199	
N stage			0.037			0.204
N0	1			1		
N+	1.839	1.038–3.257		1.484	0.807–2.727	
M stage			<0.001			<0.001
M0	1			1		
M+	6.216	2.837–13.620		6.580	2.866–15.108	
TNM stage			<0.001			–
I–II	1			–	–	
III–IV	2.474	1.499–4.084		–	–	
CD163			0.019			0.141
Low	1			1		
High	2.020	1.124–3.628		1.594	0.857–2.965	
Kindlin-2			<0.001			<0.001
Low	1			1		
High	3.559	2.119–5.978		3.301	1.892–5.758	

OS, overall survival; GC, gastric cancer; HR, hazard ratio; 95% CI, 95% confidence interval.

vivo. The pre-experiment revealed that the tumorigenesis ability increased by Kindlin-2 overexpression and decreased by TGFβ inhibitor (*Supplementary Figure S3A*). In formal experiment, Kindlin-2 knockdown cells (group 02), as well as Kindlin-2 expressing cells (group 01 and group 03), were injected into the subcutaneous tissues of nude mice. Group 01 and group 02 mice received a subcutaneous injection of TGFβ2 once a week, while group 03 mice received an injection of SB431542. Tumor volumes and body weight were measured and recorded three times per week (*Figure 5B*). When the average tumor size reached 2,000 mm^3, the mice were sacrificed, and the volume and weight of tumors were examined. Tumors formed in all mice, but tumors in group 01 (TGFβ2/Kindlin-2$^+$group) were larger (2,251.38±469.10 mm^3 *vs.* 1,530.63±627.78 mm^3, P=0.045; 2,251.38±469.10 mm^3 *vs.* 380.43±23.28 mm^3, P<0.001) and heavier (1,468.35±358.73 mg *vs.* 948.10±443.81 mg, P=0.047; 1,468.35±358.73 mg *vs.* 468.19±45.11 mg, P<0.001) than other groups (group 02, TGFβ2/Kindlin-2$^-$ group; group 03, SB431542/Kindlin-2$^+$group) (*Figure 5C*). The tumors were also examined by hematoxylin and eosin (HE) staining (*Figure 5D*), and immunohistochemistry (IHC) staining in the border of tumors showed that the expression of several invasion-related markers was significantly different in group 01 compared with group 02 (*Supplementary Figure S3B*). Two mice in group 01 exhibited suspected nodes in the lung, but they were not confirmed as metastatic tumors by HE staining (*Supplementary Figure S3C,D*).

Discussion

TAMs are abundant in the tumor microenvironment and play important roles in tumor progression (18). Recent

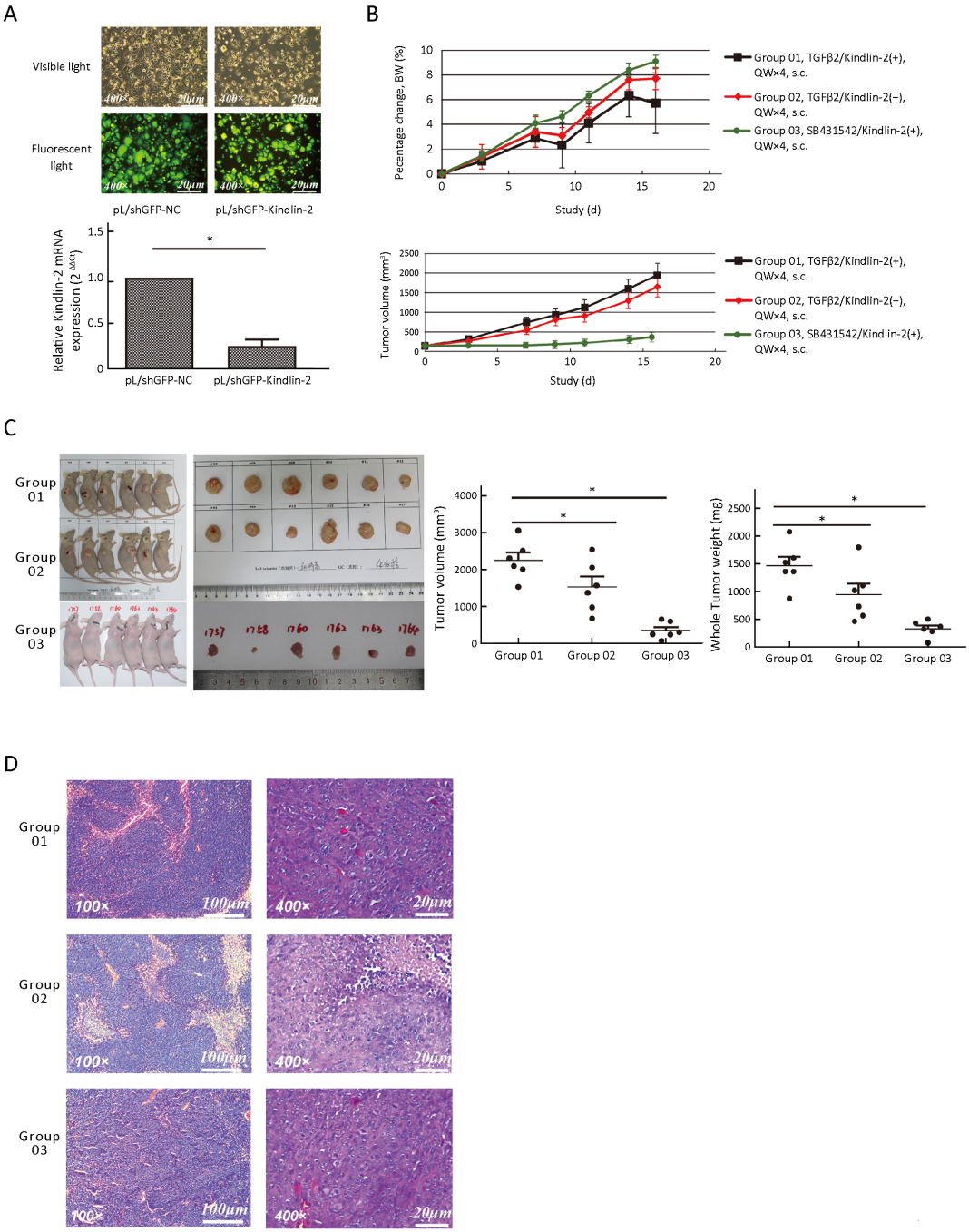

Figure 5 Invasion mechanisms were verified *in vivo* in a nude mouse oncogenesis model. (A) Green fluorescence was observed under a fluorescence microscope in the stably transfected Kindlin-2 knockdown group. Kindlin-2 expression was significantly higher in the stably transfected group than in the negative control group (×400); (B) Tumor volumes and body weights were measured and recorded three times per week; (C) When the average tumor size reached 2,000 mm^3, the mice were sacrificed, and the volume and weight of tumors were examined. Tumors formed in all mice, but the tumors in group 01 (TGFβ2/Kindlin-2$^+$group) were larger (2,251.38±469.10 mm^3 *vs.* 1,530.63±627.78 mm^3, P=0.045; 2,251.38±469.10 mm^3 *vs.* 380.43±23.28 mm^3, P<0.001) and heavier (1,468.35±358.73 mg *vs.* 948.10±443.81 mg, P=0.047; 1,468.35±358.73 mg *vs.* 468.19±45.11 mg, P<0.001) than those in the other groups (group 02, TGFβ2/Kindlin-2$^-$ group; group 03, SB431542/Kindlin-2$^+$group); (D) Tumors were examined by hematoxylin and eosin (HE) staining (×400). TGFβ2, transforming growth factor β2. *, P<0.05.

studies have shown that TAMs develop from macrophages stimulated with CSF-1, CCL2, VEGF, IL-10, IL-6 and other factors secreted by tumor cells (19-22); in turn, TAMs inhibit the immune response and promote tumor angiogenesis (23). Moreover, chronic inflammation mediated by TAMs is closely related to tumor invasion and metastasis (24). Schmieder *et al*. found that M2 macrophages play a positive role in tumor progression (25) and Yan *et al*. demonstrated that high level of TAM infiltration is related to aggressive characteristics and is an independent prognostic factor in GC (26). In our study, we successfully induced the differentiation of M1 macrophages and M2 macrophages. We identified M2 macrophages as TAMs by flow cytometry: CD163, CD206, CD11b are highly expressed on M2 macrophages (27,28), and CD86 is substantially expressed on M1 macrophages (29).

TGFβ2 belongs to a multifunctional transforming growth factor superfamily that regulates cell growth, differentiation and matrix production (30,31). High TGFβ2 expression correlates with malignancy in many cancers (32). NF-κB, a multisubunit eukaryotic transcription factor consisting of either homo- or heterodimers of various members of the Rel family, such as p50, p52, p65 (RelA), c-Rel and RelB (33), participates in a major pathway mediating a complex of matrix metalloproteinases and inflammatory factors and plays important roles in DNA transcription, cytokine production, cell survival, and inflammatory responses (34,35). Furthermore, several studies have demonstrated that NF-κB is involved in many signaling pathways active in various cancers (36-38). Our previous study found that the expression of TGFβ2 was significantly increased when GC cells were cocultured with TAMs. Our current study reported that TGFβ2 could increase the invasive ability of GC cells through promoting Kindlin-2 expression. Furthermore, we explored the binding sites of the transcription factor NF-κB in the *Kindlin-2* gene promoter region using dual-luciferase and ChIP assays. Several studies have shown that Kindlin-2 interacts with numerous signaling pathways, such as the Wnt/β-catenin (39), TGFβ/Smad (40) and TGFβ-HOXB9-paxillin signaling pathway (41). To the best of our knowledge, this study first reported the role of TGFβ2/NF-κB/Kindlin-2 signaling axis influencing cancer progression.

The deregulation of Kindlin-2 is associated with prognosis in various human cancers (42,43). Our study examined four typical markers of tumor microenvironment to establish their pathological significance and clinical relevance in GC patients. We found that CD163 and Kindlin-2 protein levels were higher in GC tumor tissues than normal tissues and that CD163 (cut-off value=3), TGFβ2 (cut-off value=3) and Kindlin-2 (cut-off value=4) could most significantly distinguish the outcomes of these GC patients. We noticed there was no significant difference in TGFβ2 between tumor and normal tissues, and the difference in Kindlin-2 expression was modest, although both had remarkable effects on survival time. To explain these observations, we noticed that the data used for the survival related analysis were only the scores for TGFβ2/Kindlin-2 in tumor tissues, and the expression analysis compared the difference between tumor and normal tissues. Moreover, the analysis of different expressions focused mainly on determining whether the marker could be used for diagnosis, while the survival analysis aimed to determine whether the marker could be used for judging prognosis; interaction might exist between them, but the relationship was not absolute. A future in-depth study with a larger sample size will be required to explore the potential reasons. Through univariate analysis, we found that high expression of CD163 and Kindlin-2 was positively associated with higher TNM stage and reduced OS. Additionally, the multivariate analysis indicated that Kindlin-2 was an independent prognostic parameter for OS. Hence, we demonstrated that Kindlin-2 could be an appropriate biomarker for GC detection and outcome prediction.

Integrins are obligate heterodimers composed of α and β subunits (44). Many studies have shown that integrins can considerably affect the survival, growth, proliferation, differentiation, invasion and metastasis of tumor cells through various pathways (45,46). Kindlin-2 has been reported to play a crucial role in the activation of β1 and β3 integrins through enhancing integrin phosphorylation (47). Several studies have suggested that integrin expression is related to NF-κB activation. For example, Lamb *et al*. (48) showed that the upregulation of integrin α6β1 increased NF-κB activation in prostate cancer. In addition, Kiefel *et al*. (49) found that the interaction of integrin α5 with the L1 cell adhesion molecule resulted in the constitutive activation of NF-κB in pancreatic adenocarcinoma cells. We found that NF-κB can promote the expression of Kindlin-2. If Kindlin-2 can phosphorylate integrins and subsequently activate NF-κB, a regulatory feedback mechanism might exist among NF-κB, Kindlin-2 and integrin. However, further study is needed to confirm this hypothesis.

Conclusions

We report a novel finding that Kindlin-2 is highly expressed in GC and is positively associated with GC cell invasion and metastasis. Further findings demonstrated that TAMs participate in the progression of GC through the TGFβ2/NF-κB/Kindlin-2 axis, and that Kindlin-2 is a novel putative target for the treatment of GC. This work strengthens the general link between Kindlin-2 expression and malignancy, thus creating new options and approaches for further investigation.

Acknowledgements

This study was supported by grants from the National Natural Science Foundation of China (No. 81372291).

Footnote

Conflicts of Interest: The authors have no conflicts of interest to declare.

References

1. Bray F, Ferlay J, Soerjomataram I, et al. Global cancer statistics 2018: GLOBOCAN estimates of incidence and mortality worldwide for 36 cancers in 185 countries. CA Cancer J Clin 2018;68:394-424.
2. Lordick F, Allum W, Carneiro F, et al. Unmet needs and challenges in gastric cancer: the way forward. Cancer Treat Rev 2014;40:692-700.
3. Yang L, Zheng R, Wang N, et al. Incidence and mortality of stomach cancer in China, 2014. Chin J Cancer Res 2018;30:291-8.
4. Catalano V, Labianca R, Beretta GD, et al. Gastric cancer. Crit Rev Oncol Hematol 2009;71:127-64.
5. Zhang G, Zhao X, Li J, et al. Racial disparities in stage-specific gastric cancer: analysis of results from the Surveillance Epidemiology and End Results (SEER) program database. J Investig Med 2017;65: 991-8.
6. Smith HA, Kang Y. The metastasis-promoting roles of tumor-associated immune cells. J Mol Med (Berl) 2013;91:411-29.
7. Mantovani A, Allavena P, Sica A., et al Cancer-related inflammation. Nature 2008;454:436-44.
8. Seoane S, Martinez-Ordoñez A, Eiro N, et al. POU1F1 transcription factor promotes breast cancer metastasis via recruitment and polarization of macrophages. J Pathol 2019;249:381-94.
9. Lin C, He H, Liu H, et al. Tumour-associated macrophages-derived CXCL8 determines immune evasion through autonomous PD-L1 expression in gastric cancer. Gut 2019;68:1764-73.
10. Zhao C, Lu X, Bu X, et al. Involvement of tumor necrosis factor-alpha in the upregulation of CXCR4 expression in gastric cancer induced by *Helicobacter pylori*. BMC Cancer 2010;10:419.
11. Tu Y, Wu S, Shi X, et al. Migfilin and Mig-2 link focal adhesions to filamin and the actin cytoskeleton and function in cell shape modulation. Cell 2003;113: 37-47.
12. Montanez E, Ussar S, Schifferer M, et al. Kindlin-2 controls bidirectional signaling of integrins. Genes Dev 2008;22:1325-30.
13. Shen Z, Ye Y, Dong L, et al. Kindlin-2: a novel adhesion protein related to tumor invasion, lymph node metastasis, and patient outcome in gastric cancer. Am J Surg 2012;203:222-9.
14. Gilmore TD. Introduction to NF-κB: players, pathways, perspectives. Oncogene 2006;25:6680-4.
15. Kang HJ, Eo SH, Kim SC, et al. Increased number of metastatic lymph nodes in adenocarcinoma of the ampulla of Vater as a prognostic factor: a proposal of new nodal classification. Surgery 2014;155:74-84.
16. Palumbo A, Avet-Loiseau H, Oliva S, et al. Revised international staging system for multiple myeloma: A report from International Myeloma Working Group. J Clin Oncol 2015;33:2863-9.
17. Wang C, Huang XF, Cai QQ, et al. Prognostic study for overall survival in patients with newly diagnosed POEMS syndrome. Leukemia 2017;31:100-6.
18. Goswami KK, Ghosh T, Ghosh S, et al. Tumor promoting role of anti-tumor macrophages in tumor microenvironment. Cell Immunol 2017;316:1-10.
19. Ryder M, Gild M, Hohl TM, et al. Genetic and pharmacological targeting of CSF-1/CSF-1R inhibits tumor-associated macrophages and impairs BRAF-induced thyroid cancer progression. PLoS One 2013;8:e54302.
20. Yang C, He L, He P, et al. Increased drug resistance in breast cancer by tumor-associated macrophages through IL-10/STAT3/bcl-2 signaling pathway. Med Oncol 2015;32:352.

21. Hutchins AP, Poulain S, Miranda-Saavedra D. Genome-wide analysis of STAT3 binding *in vivo* predicts effectors of the anti-inflammatory response in macrophages. Blood 2012;119:e110-119.
22. Mauer J, Chaurasia B, Goldau J, et al. Signaling by IL-6 promotes alternative activation of macrophages to limit endotoxemia and obesity-associated resistance to insulin. Nat Immunol 2014;15:423-30.
23. Mantovani A, Sozzani S, Locati M, et al. Macrophage polarization: tumor-associated macrophages as a paradigm for polarized M2 mononuclear phagocytes. Trends Immunol 2002;23:549-55.
24. Zeisberger SM, Odermatt B, Marty C, et al. Clodronate-liposome-mediated depletion of tumour-associated macrophages: a new and highly effective antiangiogenic therapy approach. Br J Cancer 2006;95:272-81.
25. Schmieder A, Michel J, Schönhaar K, et al. Differentiation and gene expression profile of tumor-associated macrophages. Semin Cancer Biol 2012;22: 289-97.
26. Yan Y, Zhang J, Li JH, et al. High tumor-associated macrophages infiltration is associated with poor prognosis and may contribute to the phenomenon of epithelial-mesenchymal transition in gastric cancer. Onco Targets Ther 2016;9:3975-83.
27. Barros MH, Hauck F, Dreyer JH, et al. Macrophage polarisation: an immunohistochemical approach for identifying M1 and M2 macrophages. PLoS One 2013;8:e80908.
28. Furudate S, Fujimura T, Kambayashi Y, et al. Comparison of $CD163^+$ $CD206^+$ M2 macrophages in the lesional skin of bullous pemphigoid and pemphigus vulgaris: the possible pathogenesis of bullous pemphigoid. Dermatology 2014;229:369-78.
29. Dong P, Ma L, Liu L, et al. $CD86^+$/$CD206^+$, diametrically polarized tumor-associated macrophages, predict hepatocellular carcinoma patient prognosis. Int J Mol Sci 2016;17:320.
30. Seoane J, Gomis RR. TGF-β family signaling in tumor suppression and cancer progression. Cold Spring Harb Perspect Biol 2017;9:pii:a022277.
31. Massagué J. TGF-β signal transduction. Annu Rev Biochem 1998;67:753-91.
32. Massagué J, Blain SW, Lo RS. TGFβ signaling in growth control, cancer, and heritable disorders. Cell 2000;103:295-309.
33. Karin M, Ben-Neriah Y. Phosphorylation meets ubiquitination: the control of NF-κB activity. Annu Rev Immunol 2000;18:621-63.
34. Tian B, Brasier AR. Identification of a nuclear factor kappa B-dependent gene network. Recent Prog Horm Res 2003;58:95-130.
35. Brasier AR. The NF-κB regulatory network. Cardiovasc Toxicol 2006;6:111-30.
36. Senftleben U, Cao Y, Xiao G, et al. Activation by IKKα of a second, evolutionary conserved, NF-κB signaling pathway. Science 2001;293:1495-9.
37. Vlahopoulos SA, Cen O, Hengen N, et al. Dynamic aberrant NF-κB spurs tumorigenesis: a new model encompassing the microenvironment. Cytokine Growth Factor Rev 2015;26:389-403.
38. Escárcega RO, Fuentes-Alexandro S, Garcia-Carrasco M, et al. The transcription factor nuclear factor-kappa B and cancer. Clin Oncol (R Coll Radiol) 2007;19: 154-61.
39. Yu Y, Wu J, Wang Y, et al. Kindlin 2 forms a transcriptional complex with β-catenin and TCF4 to enhance Wnt signalling. EMBO Rep 2012;13:750-8.
40. Wei X, Xia Y, Li F, et al. Kindlin-2 mediates activation of TGF-β/Smad signaling and renal fibrosis. J Am Soc Nephrol 2013;24:1387-98.
41. Zhan J, Song J, Wang P, et al. Kindlin-2 induced by TGF-β signaling promotes pancreatic ductal adenocarcinoma progression through downregulation of transcriptional factor HOXB9. Cancer Lett 2015;361: 75-85.
42. Lin J, Lin W, Ye Y, et al. Kindlin-2 promotes hepatocellular carcinoma invasion and metastasis by increasing Wnt/β-catenin signaling. J Exp Clin Cancer Res 2017;36:134.
43. Yoshida N, Masamune A, Hamada S, et al. Kindlin-2 in pancreatic stellate cells promotes the progression of pancreatic cancer. Cancer Lett 2017;390:103-14.
44. Takada Y, Ye X, Simon S. The integrins. Genome Biol 2007;8:215.
45. Shannon KE, Keene JL, Settle SL, et al. Anti-metastatic properties of RGD-peptidomimetic agents S137 and S247. Clin Exp Metastasis 2004;21:129-38.
46. Baronas-Lowell D, Lauer-Fields JL, Borgia JA, et al. Differential modulation of human melanoma cell metalloproteinase expression by α2β1 integrin and

CD44 triple-helical ligands derived from type IV collagen. J Biol Chem 2004;279:43503-13.
47. Kikkawa Y, Sanzen N, Fujiwara H, et al. Integrin binding specificity of laminin-10/11: laminin-10/11 are recognized byalpha 3 beta 1, alpha 6 beta 1 and alpha 6 beta 4 integrins. J Cell Sci 2000;113:869-76.
48. Lamb LE, Zarif JC, Miranti CK. The androgen receptor induces integrin α6β1 to promote prostate tumor cell survival via NF-κB and Bcl-xL independently of PI3K signaling. Cancer Res 2011;71:2739-49.
49. Kiefel H, Bondong S, Erbe-Hoffmann N, et al. L1CAM-integrin interaction induces constitutive NF-κB activation in pancreatic adenocarcinoma cells by enhancing IL-1β expression. Oncogene 2010;29:4766-78.

Cite this article as: Wang Z, Yang Y, Cui Y, Wang C, Lai Z, Li Y, Zhang W, Mustonen H, Puolakkainen P, Ye Y, Jiang K, Shen Z, Wang S. Tumor-associated macrophages regulate gastric cancer cell invasion and metastasis through TGFβ2/NF-κB/Kindlin-2 axis. Chin J Cancer Res 2020;32(1):72-88. doi: 10.21147/j.issn.1000-9604.2020.01.09

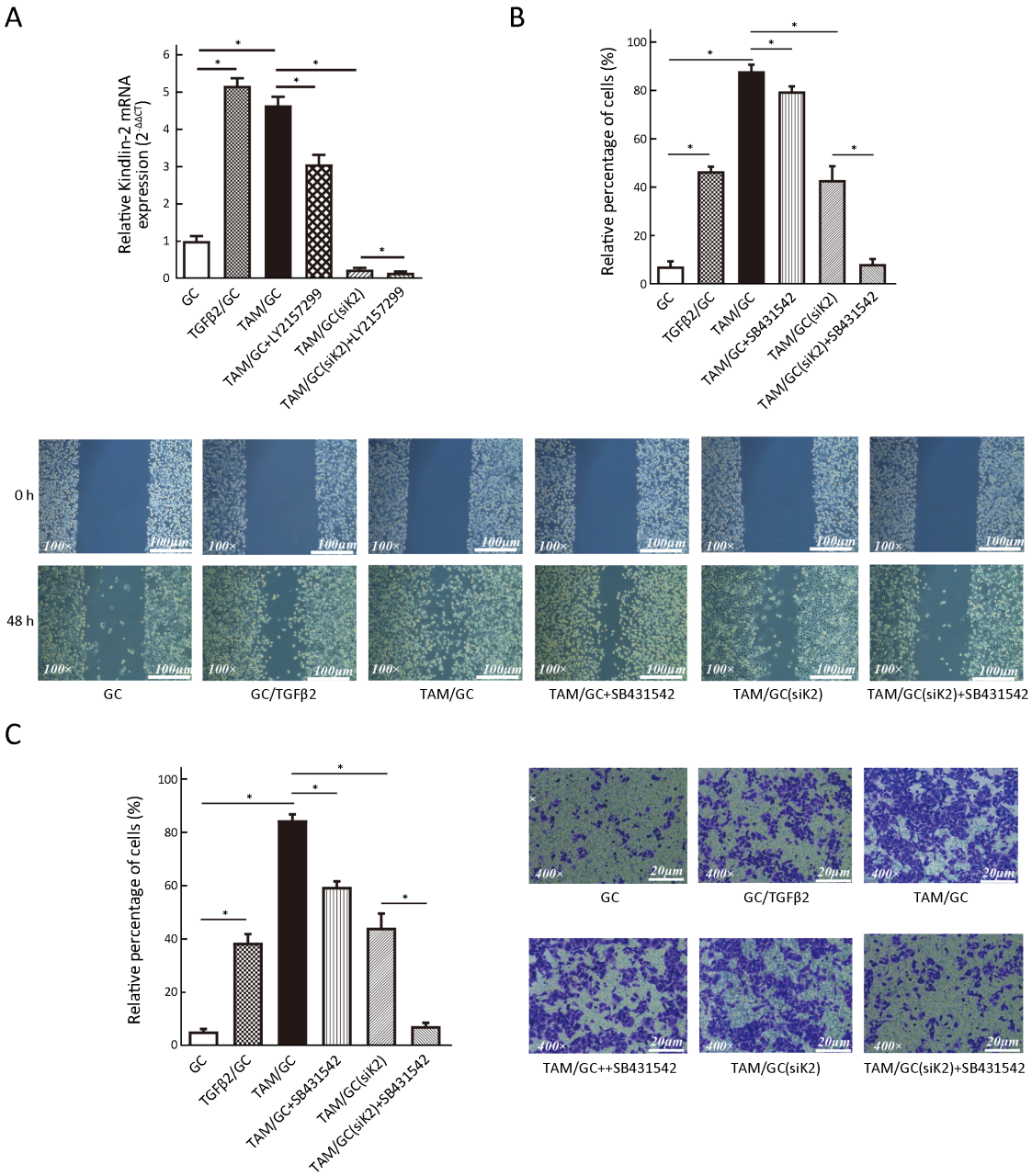

Figure S1 Comparison of Kindlin-2 expression or cell invasive ability among different groups. (A) Comparison of Kindlin-2 mRNA expression among GC, TAM/GC, TAM/GC(siK2), TGFβ2/GC, TAM/GC+LY2157299, and TAM/GC(siK2)+LY2157299 groups of cells. (GC, 0.98±0.04; TAM/GC, 4.54±0.08; TAM/GC(siK2), 0.32±0.02; TGFβ2/GC, 5.14±0.11; TAM/GC+LY2157299, 0.28±0.12 and TAM/GC(siK2)+LY2157299, 0.27±0.01, P<0.001); (B) Scratch assay comparing the cell invasive ability among GC, TAM/GC, TAM/GC(siK2), TGFβ2/GC, TAM/GC+SB431542, and TAMs/GC(siK2)+SB431542 groups of cells [GC, (8.3±2.1)%; TAM/GC, (83.3±3.9)%; TAM/GC(siK2), (43.2±7.2)%; TGFβ2/GC, (44.3±1.9)%; TAM/GC+SB431542, (78.3±2.9)% and TAMs/GC (siK2)+SB431542, (9.3±2.0)%, P<0.001] (×100); (C) Using migration assay to compare the cell invasive ability among GC, TAM/GC, TAM/GC(siK2), TGFβ2/GC, TAM/GC+SB431542, and TAMs/GC(siK2)+SB431542 groups of cells [GC, (5.8±1.1)%; TAM/GC, (84.3±2.9)%; TAM/GC(siK2), (40.2±7.4)%; TGFβ2/GC, (38.3±3.7)%; TAM/GC+SB431542, (58.3±3.1)% and TAMs/GC(siK2)+SB431542, (9.6±1.7)%, P<0.001] (×400). GC, gastric cancer; TGFβ2, transforming growth factor β2; TAM, tumor-associated macrophage. *, P<0.05.

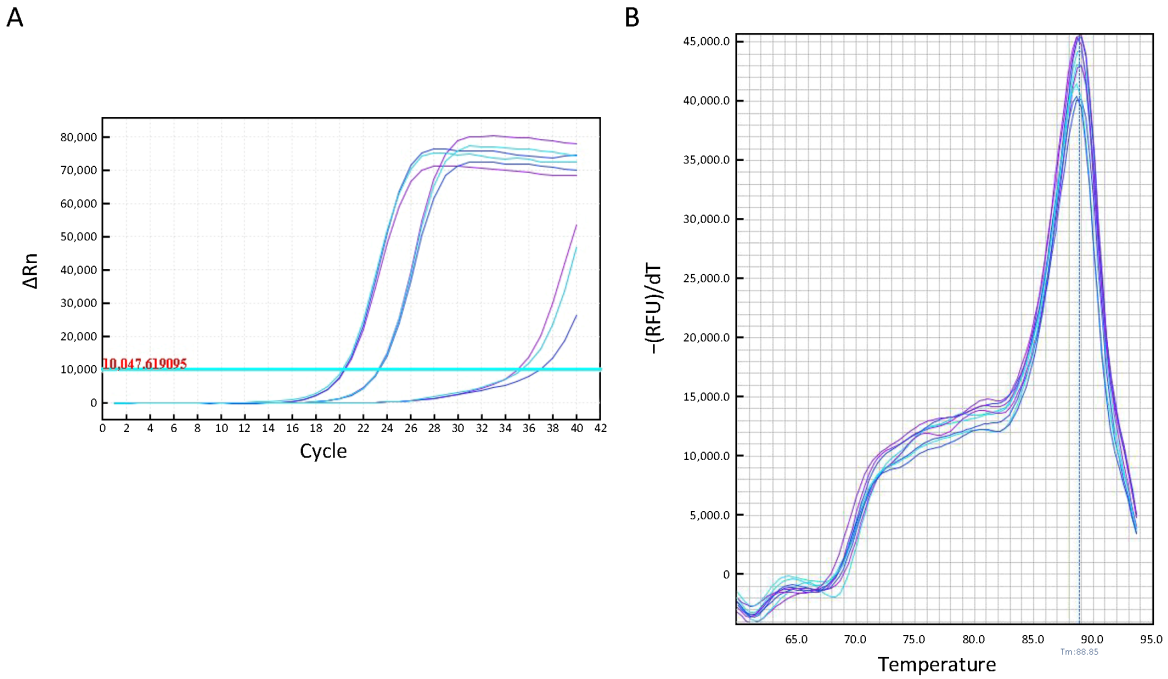

Figure S2 Amplification curve and melting curve of chromatin immunoprecipitation (ChIP) assay. (A) Amplification curve of ChIP assay; (B) Melting curve of ChIP assay.

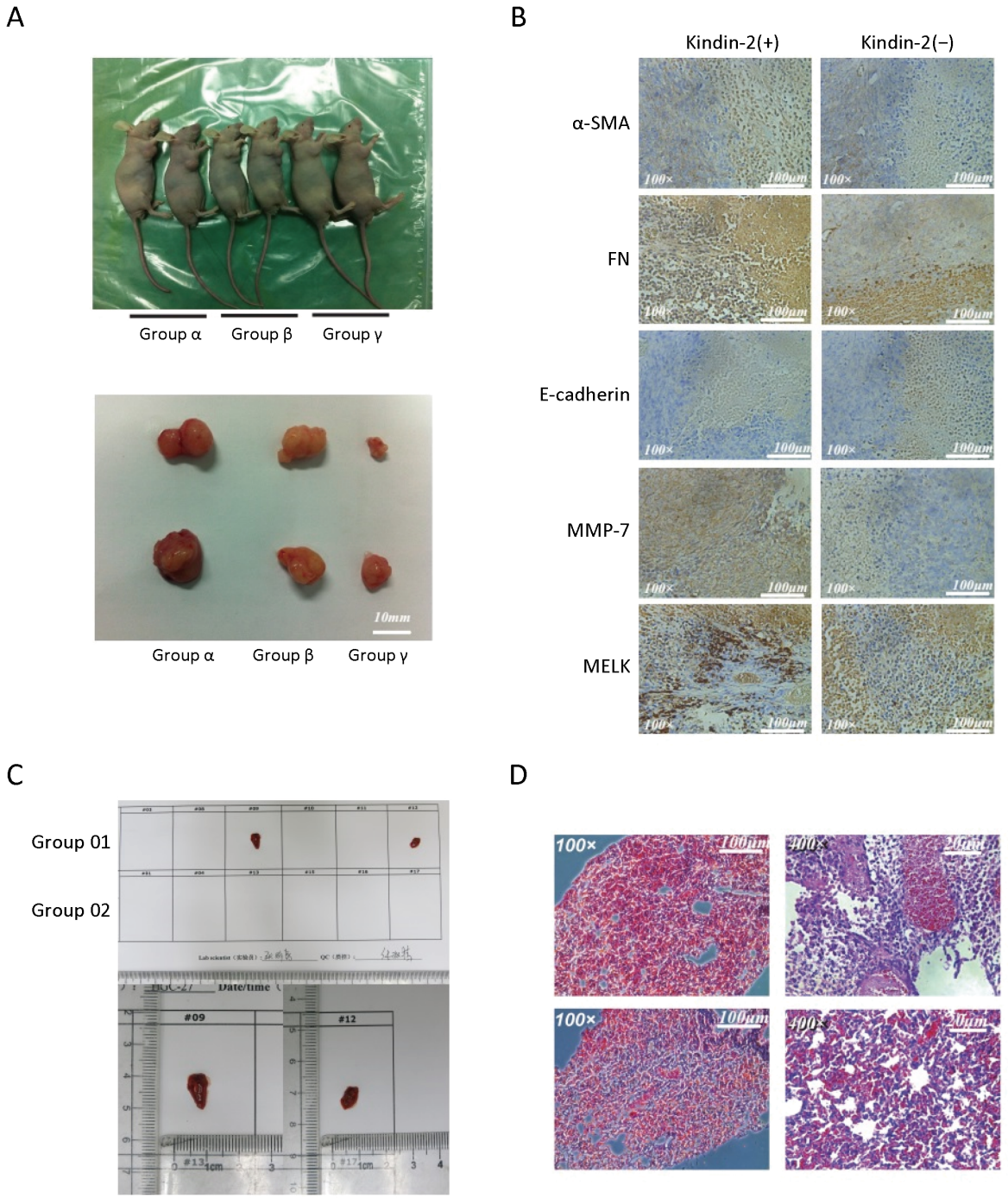

Figure S3 Evaluation of tumorigenesis abilities in preliminary experiments, and study of pulmonary nodules in formal experiments. (A) Different tumorigenesis abilities were tested in three groups, Kindlin-2 overexpression group, Kindlin-2 normal expression group and SB431542 adding group (named group α, β and γ, respectively); (B) Immunohistochemistry (IHC) staining in the border of tumors showed several invasion-related marker proteins that were significantly different in group 01 compared with group 02 (×100); (C) Two suspected lung metastatic tumors were found in group 01 mice; (D) The suspected lung metastatic tumors were examined by hematoxylin and eosin (HE) staining (×100, ×400).

